MAGMA (2003) 16:68–76
DOI 10.1007/s10334-003-0008-6

RESEARCH ARTICLE

W. Weber-Fahr
P. Bachert
F. A. Henn
D. F. Braus
G. Ende

Signal enhancement through heteronuclear polarisation transfer in in-vivo ^{31}P MR spectroscopy of the human brain

Received: 15 July 2002
Accepted: 24 February 2003
Published online: 16 July 2003

W. Weber-Fahr (✉) · F. A. Henn · D. F. Braus · G. Ende
NMR Research in Psychiatry,
Central Institute of Mental Health,
P.O. Box 122120, 68072 Mannheim,
Germany
e-mail: wwf@skullslicer.zi-mannheim.de
Tel.: +49-621-1703669
Fax: +49-621-1703673

P. Bachert
Department of Biophysics
and Medical Radiation Physics,
German Cancer Research Center (DKFZ),
Heidelberg, Germany

Abstract Significant ^{31}P NMR signal enhancement through heteronuclear polarisation transfer was obtained in model solutions and in vivo on a 1.5-T whole-body MR scanner equipped with two RF channels. The much higher population differences involved in proton Zeeman energy levels can be transferred to the ^{31}P levels with the refocused INEPT (insensitive nucleus enhancement by polarisation transfer) double-resonance experiment by means of a series of simultaneously applied broadband RF pulses. INEPT achieves a polarisation transfer from ^{1}H to ^{31}P spin states by directly reordering the populations in spin systems with heteronuclear scalar coupling. Thus, only the ^{31}P NMR signal of metabolites with scalar ^{1}H–^{31}P coupling is amplified, while the other metabolite signals in the spectra are suppressed. Compared to Ernst-angle excitation, a repetition-time-dependent signal enhancement of η=(29±3)% for methylene diphosphonic acid (MDPA) and η=(56±1)% for phosphorylethanolamine (PE) was obtained on model solutions through optimisation of the temporal parameters of the pulse experiment. The results are in good agreement with numerical calculations of the theoretical model for the studied spin systems. With optimised echo times, in-vivo ^{31}P signal enhancement of the same order was obtained in studies of the human brain.

Keywords ^{31}P MR spectroscopy · Polarisation transfer · INEPT · Human brain · In vivo

Introduction

The application of in-vivo ^{31}P MR spectroscopy (^{31}P MRS) in clinical routine is limited by the low signal-to-noise ratio (S/N) at B_0=1.5 T, which leads to long measurement times, poor spatial resolution, and difficult quantitative evaluation of ^{31}P spectra. Additionally, the broad signal of phospholipids, which interferes with the resonances of other metabolites in the in-vivo ^{31}P MR spectrum, complicates the post-processing.

Established techniques to improve S/N and spectral quality of ^{31}P MRS refer to ^{1}H–^{31}P double resonance, i.e., {^{1}H}–^{31}P nuclear Overhauser effect (NOE) and ^{1}H-decoupling. The NOE is bound to dipolar-coupled spins in liquid phase. The signal enhancement for metabolites with scalar ^{1}H–^{31}P couplings can be further increased, e.g. by means of the INEPT (insensitive nucleus enhancement by polarisation transfer) technique. The much higher population differences involved in proton Zeeman energy levels can be transferred to the ^{31}P levels with INEPT by means of a series of broadband RF pulses applied simultaneously with appropriate phases. INEPT achieves a polarisation transfer from ^{1}H to ^{31}P spin states by directly reordering the populations in spin systems with heteronuclear scalar coupling. Thus, only the ^{31}P MR signal of metabolites with scalar ^{1}H–^{31}P couplings [namely, phosphomonoester (PME) and phosphodiester (PDE)] is amplified, while the other metabolite signals in the spectra are suppressed.

INEPT is known in high-resolution MR spectroscopy, but, to our knowledge, has only been applied in two in-vivo ^{31}P MRS studies [1, 2]. The difficulties with this

application arise from the weak phosphorus-proton J-couplings (J_{AK}~4–8 Hz), which require long echo times, and the relatively short T_2 relaxation times of ^{31}P metabolites with ^{31}P–^{1}H coupling (11 ms–100 ms) [3, 4]. We therefore explored the theoretical and experimental implications of heteronuclear polarisation transfer (PT) in in-vivo {^{1}H}–^{31}P MRS on a 1.5-T whole-body MR scanner with the ultimate goal of obtaining a most effective refocused INEPT (RINEPT) sequence for ^{31}P signal amplification in MRS studies of the human brain.

PME and PDE are intermediates of membrane phospholipid turnover and thus their resonances are of interest in many brain diseases that involve membrane defects. For the PDE resonance, a correlation with peripheral measures of the highly unsaturated fatty acids docosahexaenoic acid and eicosapentaenoic acid has recently been shown [5].

Theory

The intensities of MR-detectable resonances are proportional to the population differences of the Zeeman energy levels of the observed spin system. In a coupled system of different nuclei, e.g. sensitive nuclei A and insensitive nuclei K (with gyromagnetic ratios $\gamma_A > \gamma_K$), there are large variations of the population differences of the energy levels depending on the ratio γ_A/γ_K. Resonant irradiation of one spin species affects the populations of the states of the other. Polarisation transfer can occur when the connectivity of the different spins in a coupled system allows the population differences of the sensitive nuclei to be transferred to the ensemble of insensitive nuclei.

Figure 1 shows the pulse sequence of the {^{1}H}–^{31}P RINEPT experiment [6, 7]. The first part is the "classical" INEPT sequence. The RF pulses applied at ^{1}H and ^{31}P frequencies basically invert the population differences of the Zeeman levels along specific A-nucleus transitions. This is accomplished after the evolution time TE_1=1/(2J) and the simultaneous 90° pulses (Fig. 1, time point 2). The final simultaneous 180° pulses (which expand the INEPT to the RINEPT experiment) refocus transversal magnetisation components depending on the echo time TE_2. TE_2 determines the relative phase of the coupled resonances.

In the case of a two-spin system, AK, in static magnetic field B_0, the equilibrium density operator in terms of product operators is given by:

$$\zeta_0 = p\left(\frac{\gamma_A}{\gamma_K}\mathbf{A}_z + \mathbf{K}_z\right) \tag{1}$$

where $p = \gamma_K \hbar B_0/(4k_B T$ is the population difference of K spins at thermal equilibrium (T=temperature, k_B=Boltzmann constant). After resonant irradiation of A spins, the density operator equals:

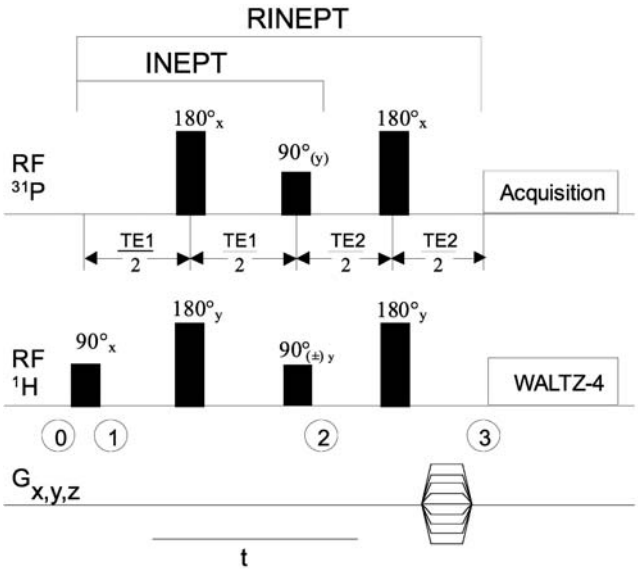

Fig. 1 {^{1}H}–^{31}P INEPT (insensitive nucleus enhancement by polarisation transfer) and refocused INEPT (RINEPT) sequence. Two spin species are excited with a sequence of rectangular RF pulses at ^{31}P and ^{1}H frequencies. The signal of the ^{31}P spins is acquired with WALTZ-4 ^{1}H-spin decoupling in the case of RINEPT. In the INEPT experiment, signal acquisition starts immediately after the simultaneous 90° pulses (time point 2). During the evolution time TE_2, gradient pulses for spatial localisation can be applied

$$\zeta_1 = \mathbf{U}^{\mathbf{A}}_{-\mathbf{90x}}\zeta_0\left[\mathbf{U}^{\mathbf{A}}_{-\mathbf{90x}}\right]^{-1} = p\left(\frac{\gamma_A}{\gamma_K}\mathbf{A}_y + \mathbf{K}_z\right) \tag{2}$$

where the operator U^A_{-90x} describes a 90°RF pulse at A-spin frequency along the negative x axis (90°$_{-x}$, Fig. 1, time point 1). Likewise, the density operator at the beginning of the acquisition phase of the INEPT experiment (Fig. 1, time point 2) reads:

$$\zeta_2[TE_1 = 1/(2J)] = p\left(\frac{\gamma_A}{\gamma_K}\mathbf{2A}_z\mathbf{K}_x - \mathbf{K}_x\right) \tag{3}$$

The expectation value of the K-spin transverse magnetisation and hence the INEPT spectrum is then directly obtained by calculating the trace of the product of density (ζ_2), Hamiltonian (U_H), and angular momentum operator ($I^K_+ = I^K_x + iI^K_y$):

$$\begin{aligned}\left\langle \overline{M^K} \right\rangle(t) &= tr\left[\mathbf{I}^{\mathbf{K}}_{+}\left(\mathbf{U_H}\zeta_2\mathbf{U}^{-1}_{\mathbf{H}}\right)\right] \\ &= \frac{p}{2}\left[\left(\frac{\gamma_A}{\gamma_K}+1\right)e^{-i(\omega_k-\pi J)t}\right. \\ &\quad \left. -\left(\frac{\gamma_A}{\gamma_K}-1\right)e^{-i(\omega_k+\pi J)t}\right].\end{aligned} \tag{4}$$

The A_zK_x magnetisation together with K_x corresponds to two resonances with relative intensities (γ_A/γ_K)+1 and

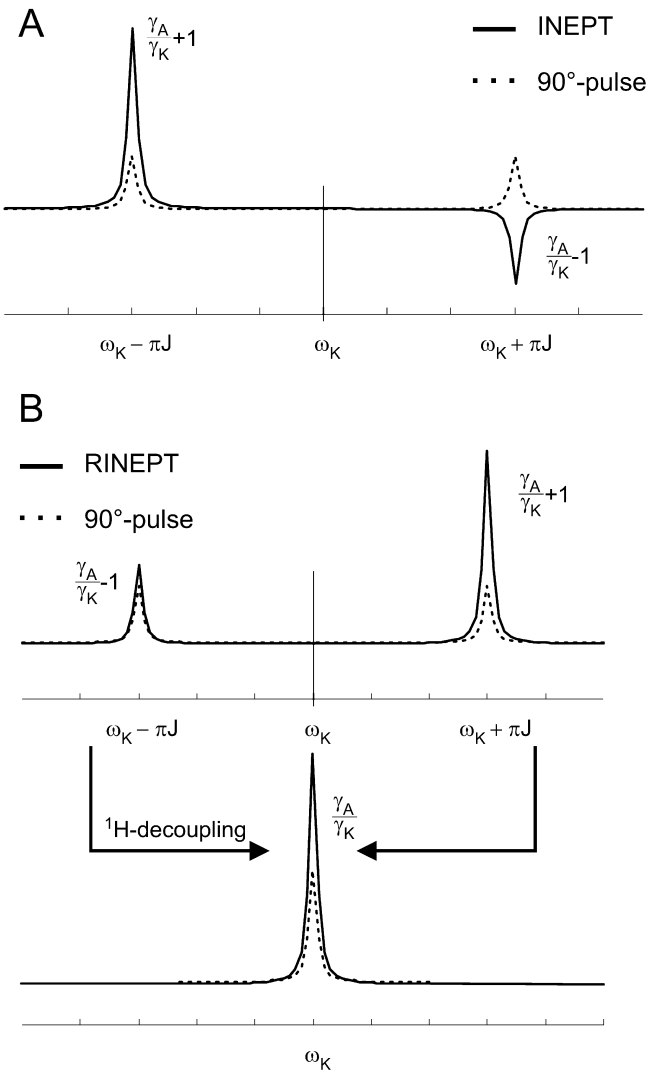

Fig. 2 Calculated ^{31}P MR spectra of {^{1}H}–^{31}P INEPT, {^{1}H}–^{31}P RINEPT, and single-pulse (90°) excitation of the ^{31}P spins in a heteronuclear two-spin system with weak scalar coupling. With INEPT, the lines of the doublet are enhanced in anti-phase configuration with $\eta=\gamma_H/\gamma_P=247\%$. Both resonances are refocused in the RINEPT experiment

$(\gamma_A/\gamma_K)-1$, demonstrating the signal enhancement of K spins achieved with INEPT (Fig. 2A).

The major disadvantage of the INEPT experiment is that proton decoupling cannot be applied because the two K-spin magnetisation components precess out of phase by 180°, hence the resulting signal will be the difference of both amplitudes. This shortcoming is solved by simultaneous irradiation of two 180° RF pulses. In this case, the density operator at echo time $TE_2=1/(2J)$ reads:

$$\zeta_3[TE_2 = 1/(2J)] = p\left(\frac{\gamma_A}{\gamma_K}\mathbf{K}_x - \mathbf{2A}_z\mathbf{K}_y\right) \tag{5}$$

The two magnetisation components refocus at time point 3 and the transverse magnetisation of K spins during the acquisition period is given by:

$$\begin{aligned}\left\langle \overline{M^K} \right\rangle (t) &= tr\left[\mathbf{I}_+^K \left(\mathbf{U}_H \zeta_3 \mathbf{U}_H^{-1}\right)\right] \\ &= -\frac{p}{2}\left[\left(\frac{\gamma_A}{\gamma_K} - 1\right) e^{-i(\omega_k - \pi J)t}\right. \\ &\quad \left. + \left(\frac{\gamma_A}{\gamma_K} + 1\right) e^{-i(\omega_k + \pi J)t}\right].\end{aligned} \tag{6}$$

Upon ^{1}H-decoupling during the acquisition phase of the K-spin magnetisation, both resonance lines will collapse to a single line and the overall signal enhancement of the RINEPT sequence through polarisation transfer in a weakly coupled system of one ^{31}P nucleus and one proton is given by:

$$\eta = \frac{M^K}{M_0} - 1 = \frac{\gamma_A}{\gamma_K} - 1 = 147\ \% \tag{7}$$

with the thermal equilibrium magnetisation M_0. For complex molecules with more than two interacting spins the theory becomes more complicated. The coherence transfer and the refocusing of the different magnetisation components may not be perfect and the signal enhancements and optimum echo times may vary.

Since the signal obtained in a RINEPT experiment depends on the transfer of coherence rather then on excited magnetisation from thermal equilibrium, the repetition time of the experiment is determined mainly by the T_1 relaxation time of the sensitive spins. In the case of ^{1}H and ^{31}P, T_1 of the less sensitive ^{31}P spins is much longer than that for the protons. This difference can be used to further increase the signal enhancement.

Methods

All experiments were performed on a 1.5-T whole-body MR scanner (Magnetom Vision; Siemens, Erlangen, Germany) equipped with two RF channels and a double-tuned (^{31}P/^{1}H) quadrature birdcage headcoil (∅ 29.2 cm) [8]. An anticipated difficulty of the experiment was the synchronisation of the second RF channel, which must permit simultaneous irradiation of RF pulses with definite phases in good synchronisation with the first RF channel. Because the second RF channel is only specified as a decoupler by the manufacturer, the timing of the RF pulse was verified with an oscilloscope. An unsteady time delay of up to 0.3 ms between both channels was determined.

{^{1}H}–^{31}P RINEPT studies were carried out with model solutions containing 80 mM methylene diphosphonic acid (MDPA) and 80 mM phosphorylethanolamine (PE).

In contrast to the metabolites detectable by in-vivo ^{31}P MRS, which exhibit very weak phosphorus-proton J-couplings (J_{AK}~4–8 Hz, three bond lengths), MDPA is strongly scalar coupled (J_{AK}=21 Hz, two bond lengths). Additionally, MDPA has a quite simple structure, with two protons in symmetric position relative to two ^{31}P nuclei (Fig. 3).

PE is an endogenous ^{31}P-containing metabolite with a resolved resonance in the PME region of ^{1}H-decoupled in-vivo ^{31}P MR

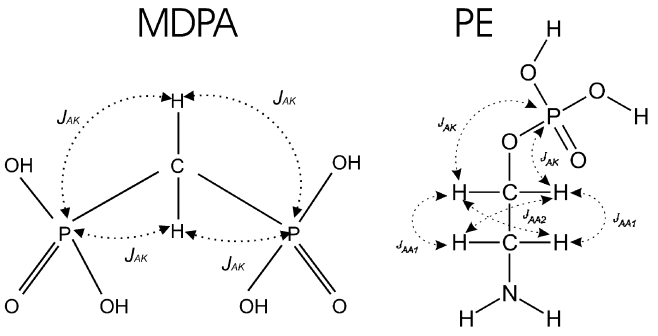

Fig. 3 Chemical structure of methylene diphosphonic acid (MDPA) and phosphorylethanolamine (PE). MDPA is a symmetric molecule with two ^{31}P nuclei that are scalar coupled over two bonds to two ^{1}H spins (J_{AK}=21 Hz). The ^{31}P spin of PE interacts over three bonds with the two protons of the first methylene group (J_{AK}=6.48 Hz). These in turn interact scalar with the protons of the second methylene group (J_{AA1}=6.9 Hz and J_{AA2}=3.25 Hz)

spectra of human brain [9]. The compound of PE with an additional glycerine group, glycerophosphorylethanolamine (GPE), resonates in the PDE region of these spectra.

The evolution of the polarisation transfer in PE is much more complicated than in MDPA because of the larger set of different *J*-couplings in PE (Fig. 3). The ^{31}P nucleus interacts with both protons of the adjacent methylene group (J_{AK}=6.5 Hz, three bond lengths). Moreover, the dynamics of the spin system are affected by homonuclear *J*-couplings of protons in the two methylene groups (J_{AA1}, J_{AA2}).

Phosphorus MR spectra of MDPA and PE aqueous solutions show a triplet with line splitting of 21 Hz and 6.5 Hz, respectively. The ^{1}H MR spectrum of MDPA exhibits the same triplet (chemical shift δ=2.3 ppm) while two multiplets centered at δ=3.27 ppm and δ=4.10 ppm arise from the methylene groups of PE. These multiplets cannot be resolved at 1.5 Tesla. High-resolution MR yields two different homonuclear coupling constants: J_{AA1}=6.9 Hz and J_{AA2}=3.25 Hz (W. Hull, DKFZ, personal communication).

The sequence parameters were optimised by first varying the echo time TE_1 in the INEPT experiment until maximum signal enhancement was obtained. In the second step, the echo time TE_2 of the RINEPT experiment was varied. An appropriate method to quantify the signal amplification with refocused INEPT is to acquire the ^{31}P signal while ^{1}H-decoupling is applied such that the multiplet structure of the differently phased signal components of the coupled spin system is removed.

To validate the measured results, the expected ^{31}P signal enhancement of the refocused INEPT experiment compared to that of 90° pulse ^{31}P excitation was calculated using the theoretical model for each spin system. The numerical calculations were made by programming the INEPT and RINEPT sequences using the GAMMA C++ libraries [10]. All coupling constants displayed in Fig. 3 were considered in the calculations. Relaxation effects were neglected in these calculations.

To study the influence of relaxation on signal enhancement, the relaxation times T_1 and T_2 of the ^{31}P spins were measured for the model solutions. Spectra were acquired with Ernst-angle excitation as well as with the refocused INEPT sequence (32 averages) and varying TR. The spectra were quantified and the ratio of the signal of RINEPT and Ernst-angle excitation (M_r/M_s) was calculated.

The RINEPT sequence was then tested in in-vivo studies with the optimised parameters. The required B_1 field for the 180° –^{31}P RF pulses was determined using a 50-ml flask filled with hexamethylphosphotriamide (HMPT) as external reference. The B_1 inhomogeneities from the fixed position of the flask to the centre of the coil were measured in phantom studies. HMPT gives a broad ^{31}P signal at 3,400 Hz up-field to the phosphocreatine (PCr) resonance; hence it does not interfere with endogeneous phosphorus resonances and can be employed in relatively high concentrations without saturating the ADC (Analogue-to-Digital Converting). The HMPT signal was also used for intersubject comparison of signal intensities in in-vivo ^{31}P spectra.

All spectra were quantified using time domain fitting with AMARES (MRUI) [11].

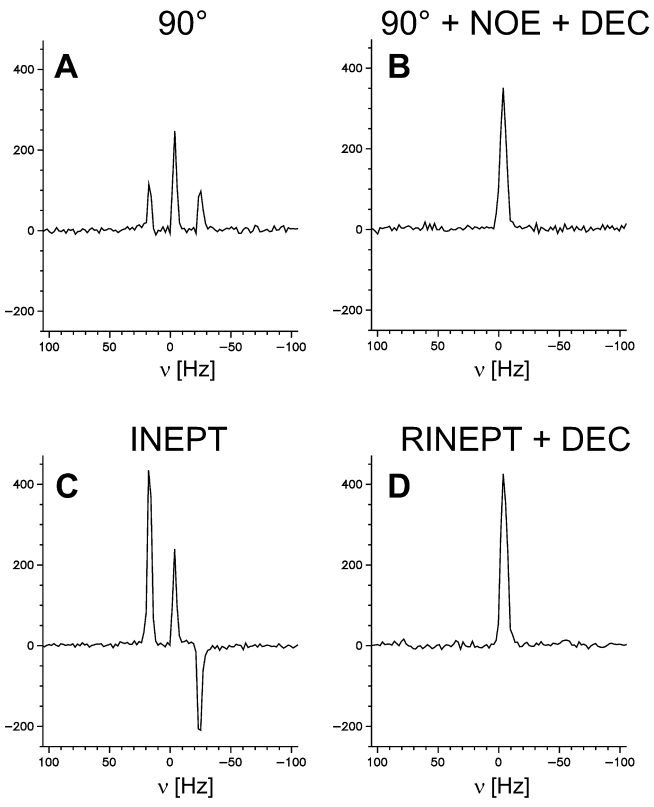

Fig. 4A–D ^{31}P MR spectra of a 80mM aqueous solution of MDPA. All spectra were obtained with the same experimental setup, *TR*=5 s, *NEX*=2, and the techniques **A** single-pulse (90°) excitation; **B** single-pulse excitation with additional NOE ^{1}H-pulse and 256-ms WALTZ-4 ^{1}H-decoupling; **C** INEPT with TE_1=12 ms; **D** RINEPT with TE_2=10 ms and 256-ms WALTZ-4 ^{1}H-decoupling

Results

Determination of TE_1, TE_2 and signal enhancements

The time parameter TE_1 for maximum polarisation transfer in the MDPA model solution was found to be TE_1= (12±1) ms≅1/(4*J*). For a system of two spins TE_1=1/(2*J*) is expected. The outer lines of the triplet are in anti-phase and enhanced depending on TE_1 (Fig. 4C). The centre line did not change compared to the single-pulse spectrum.

The optimum refocusing time was TE_2=(10±2) ms in the model solution. A refocusing of all three magnetisa-

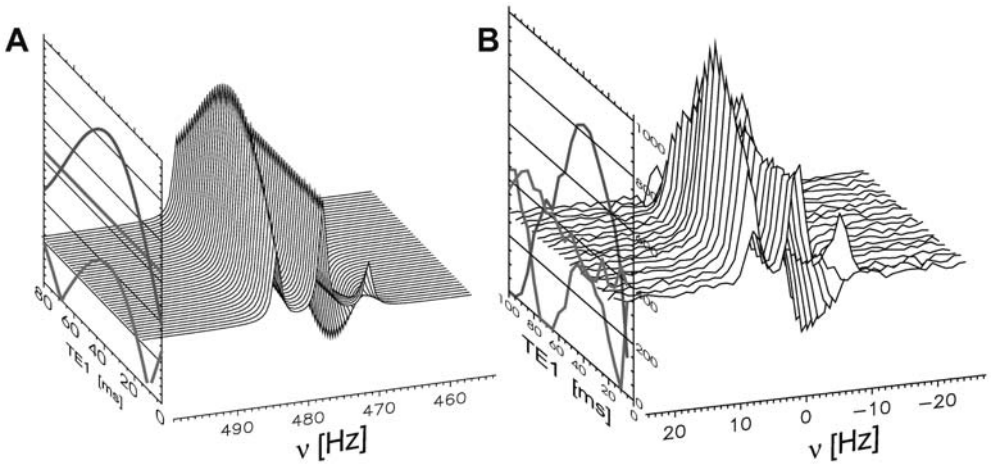

Fig. 5 Signal intensity of PE with INEPT as a function of TE_1 (0–80 ms) from **A** numerical simulation of the spin dynamics and **B** experiment. The polarisation transfer is maximum at TE_1=(40±5) ms

tion components with RINEPT is not possible in this coupled-spin system. Compared to the single-pulse spectrum, a signal enhancement of:

$$\eta = \frac{M_r}{M_s} - 1 = (29 \pm 3)\ \%$$

was measured. The results of the experiments and numerical simulations, in particular the signal enhancements, agree for the MDPA spin system.

The ^{31}P triplet resonance of PE shows the same pattern as that of MDPA when acquired with the INEPT technique, i.e. unaffected centre line and outer lines enhanced and in anti-phase configuration. Owing to the small couplings, maximum polarisation transfer was obtained with long echo time: TE_1=(40±5) ms (Fig. 5).

As in the case of the MDPA coupled-spin system, it was not possible to refocus the three magnetisation components completely with RINEPT. In the ^{1}H-decoupled RINEPT experiment with the PE model solution, a maximum ^{31}P signal enhancement of:

$$\eta = \frac{M_r}{M_s} - 1 = (22 \pm 5)\ \%$$

relative to the single-pulse spectrum was observed at TE_2=(32±5) ms (Fig. 6).

The numerical calculations for a spin system with the *J*-coupling constants valid for PE yielded TE_1=37 ms, TE_2=32 ms, and η=23%, which all are within the error range of the experimental results (Fig. 5).

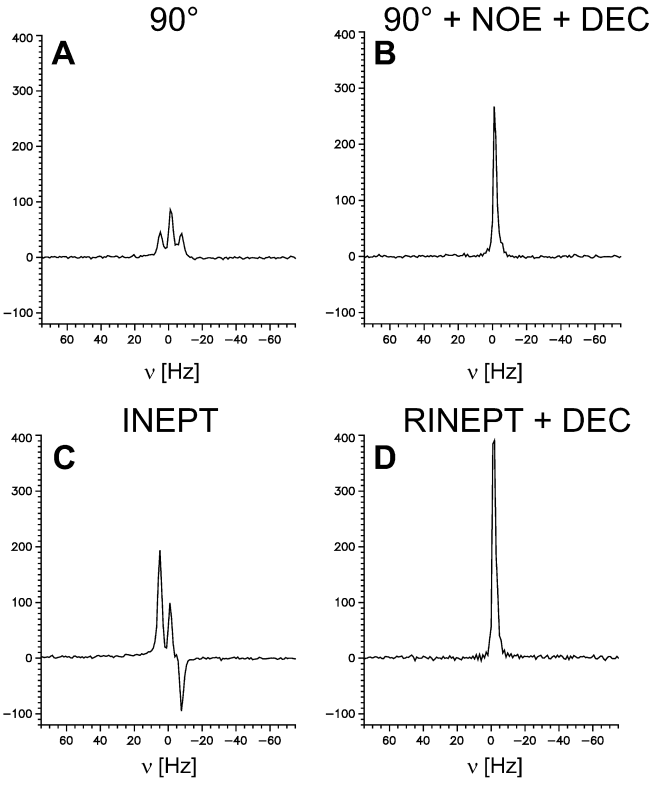

Fig. 6A–D ^{31}P MR spectra of a 80 mM aqueous solution of PE. All spectra were obtained with the same experimental setup, *TR*=8 s, *NEX*=4, and the techniques **A** single-pulse excitation; **B** single-pulse excitation with additional NOE ^{1}H-pulse and 256-ms WALTZ-4 ^{1}H-decoupling; **C** INEPT with TE_1=40 ms; **D** RINEPT with TE_2=32 ms and 256-ms WALTZ-4 ^{1}H-decoupling

Relaxation effects

The measurements of the phosphorus relaxation times in the model solutions yielded T_1^{MDPA}=(5.380±0.001) s, T_2^{MDPA}=(383.34±2.01) ms, T_1^{PE}=(8.184±0.023) s, and T_2^{PE}=(657.2±1.41) ms. Accordingly, the signal loss of 3.9% in MDPA and 4.7% in PE due to T_2 relaxation during the echo time TE_2 is smaller than the error range of the measured signal enhancement. The effect of T_1 relaxation on the signal enhancement in the RINEPT experiment compared to Ernst-angle excitation was estimated using the Ernst-angle for the measured T_1 of the PE

model solution and repetition times *TR* in the range of 1–20 s.

The expected ^{31}P signal intensity after single-pulse excitation with the Ernst-angle is given by:

$$M_s = M_0 \frac{1 - e^{-TR/T_1^P}}{\sqrt{1 - e^{-2TR/T_1^P}}} \quad (8)$$

where M_0 is the magnetisation in thermal equilibrium and $T_1{}^{\mathrm{P}}$ the ^{31}P longitudinal relaxation time. The experiments showed that the intensity of the middle line of the triplet was independent of the excitation mode. This suggests that the RINEPT signal enhancement depends not only on $T_1{}^{\mathrm{H}}$, but also on $T_1{}^{\mathrm{P}}$. Accordingly, the RINEPT signal function reported in [1] had to be extended to:

$$M_r = d_1 M_0 (1 - e^{-(TR-\delta)/T_1^H}) + d_2 M_0 (1 - e^{-TR/T_1^P}) \quad (9)$$

where d_1, d_2 quantify both the enhancement through polarisation transfer as predicted by theory ($d_1+d_2=M_r/M_0=\eta+1$ for $TR\rightarrow\infty$) and the signal contribution of the magnetisation components with different phases which depend on $T_1{}^{\mathrm{H}}$ or $T_1{}^{\mathrm{P}}$. The ^{1}H-decoupling time is taken into account by δ. Finally, with the ratio M_r/M_s from Eq. 8 and Eq. 9 we obtain the signal enhancement with RINEPT as a function of *TR*:

$$\frac{M_r}{M_s}(TR) = \frac{d_1(1 - e^{-(TR-\delta)/T_1^H}) + d_2(1 - e^{-TR/T_1^P})}{1 - e^{-TR/T_1^P}} \cdot \sqrt{1 - e^{-2TR/T_1^P}} \quad (10)$$

Figure 7 shows ratios of measured ^{31}P MR signal intensities of the PE model solution from RINEPT and single-pulse experiments as a function of *TR* (*NEX*=32). A fit of Eq. 10 to these data with use of the parameters $T_1{}^{\mathrm{P}}$=8.184 s and δ=0.5 s yielded M_r/M_0=1.219±0.050 (η=22%) and $T_1{}^{\mathrm{H}}$=(2.019±0.089) s. The plot shows, that for short *TR*, i.e. $TR\cong(1.2–2.3)\times T_1{}^{\mathrm{H}}$, M_r/M_s exceeds the theoretically predicted enhancement through polarisation transfer M_r/M_0. The fit gives a maximum at M_r/M_s= 1.560±0.001 (η=56 %).

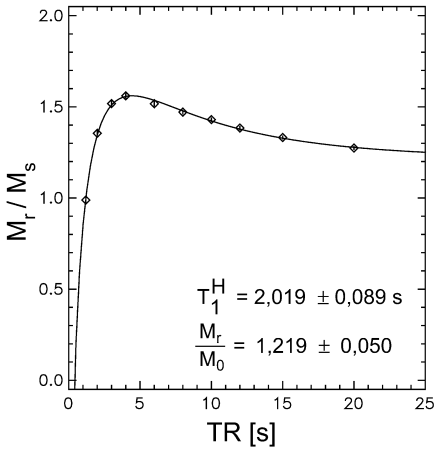

Fig. 7 ^{31}P MR signal enhancement of PE with RINEPT as a function of repetition time (TR). RINEPT (TE_1=40 ms, TE_2=32 ms, *NEX*=32) and single-pulse spectra (Ernst-angle excitation, *NEX*=32) were obtained with 500-ms WALTZ-4 ^{1}H-decoupling. The fit of Eq. 10 to the measured data points is shown

Refocused INEPT in vivo

In-vivo whole-head ^{31}P spectra of a healthy control (informed consent) were acquired using 64 averages with Ernst-angle excitation plus NOE enhancement and with RINEPT. The repetition time was set to 1.2 s, which is the minimum allowed within SAR limits when using 150 ms WALTZ ^{1}H-decoupling. With estimated ^{31}P relaxation times $T_1{}^{\mathrm{P}}$ of about 1.7–2.1 s of the phosphomono- and phosphodiesters [3, 4], the Ernst angle is 60°. The time parameters of the RINEPT sequence were set to the optimum values determined in experiments with the PE model solution: TE_1=40 ms and TE_2=32 ms.

Figure 8 shows in-vivo ^{31}P MR spectra from the brain of a volunteer. In comparison to the single-pulse spectrum (Fig. 8A), the spectrum obtained with the RINEPT sequence (Fig. 8B) is strongly simplified. The resonances of metabolites with scalar ^{1}H–^{31}P coupling (PE, GPE, GPC) are amplified while the other resonances are largely suppressed. The broad phospholipid signal has disappeared. As a consequence, post-processing of RINEPT spectra is easier, also because linear phase correction is unnecessary owing to the spin-echo character of the sequence. The signal acquired with Ernst-angle excitation always needs to be corrected for linear phase because of the hardware-dependent delay between excitation and acquisition. The delay becomes longer when phase encoding gradients have to be inserted for spatial localisation.

In spectra acquired with Ernst-angle excitation, the evaluation of signal enhancements is complicated by the broad phospholipid signal overlapping with the resonances of interest. The variance of the quantified broad resonance band from phospholipids which interferes both with PDE and PME signals is in the order of magnitude of the quantified PE, GPE and GPC resonances.

Line fitting in the time domain with AMARES (MRUI) yielded signal enhancements in the range of η=(0±14)% (PE) to η=(163±66)% (GPE).

The residual signal in the RINEPT spectra of metabolites without scalar ^{31}P–^{1}H-coupling can be completely eliminated by implementing additional phase cycling of the second 90° ^{1}H pulse and the receiver channel. Since only the phase of the signals corresponding to coupled metabolites is changed, with each following acquisition

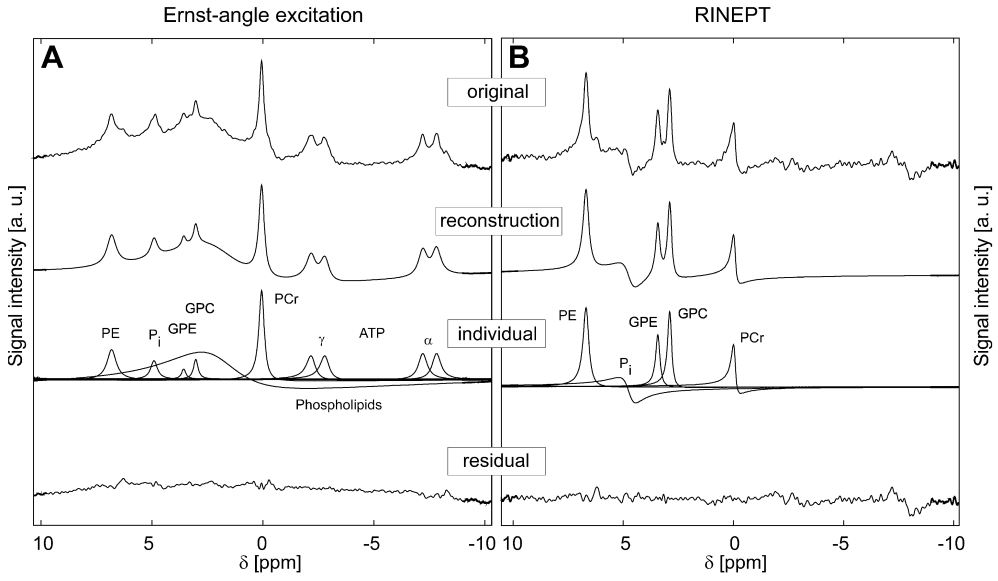

Fig. 8A, B Whole-head ^{1}H-decoupled in-vivo ^{31}P MR spectra (1.5 T, *TR*=1,200 ms, *NEX*=64) acquired in the same session. **A** Ernst-angle excitation (α=60°, NOE); **B** RINEPT (TE_1=40 ms, TE_2=32 ms). Data post-processing in the time domain with MRUI software (AMARES). Signal enhancement: η_{PE}=(0±14)%, η_{GPE}=(163±66)%, η_{GPC}=(54±22)%

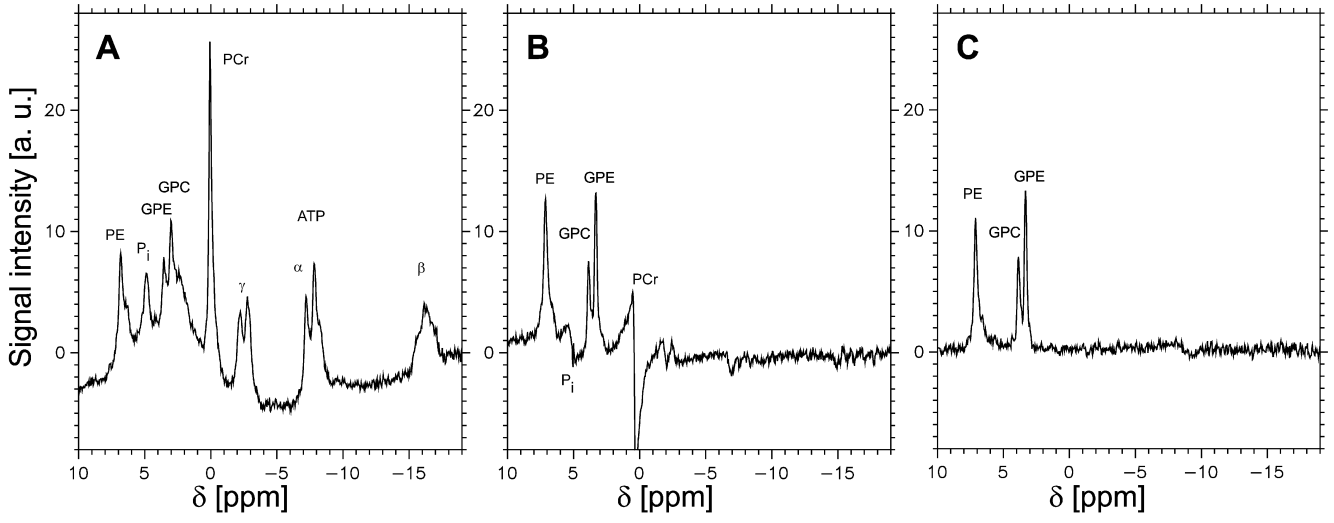

Fig. 9A–C Whole-head ^{1}H-decoupled in-vivo ^{31}P MR spectra (1.5 T, *TR*=1,200 ms, *NEX*=64) acquired in the same session. The scaling of the vertical axes is identical. **A** Ernst-angle excitation (α=60°, NOE); **B** RINEPT (TE_1=40 ms, TE_2=32 ms). Signal enhancement: η_{PE}=(55.6±8.6)%, η_{GPE}=(97.6±38.0)%, η_{GPC}=(72.6±14.1)%; **C** Experiment of **B** but with additional phase cycling. η_{PE}=(21.4±6.9)%, η_{GPE}=(79.6±33.2)%, η_{GPC}=(61.4±12.3)%

the signals of uncoupled metabolites cancel out. This is demonstrated in Fig. 9.

Even though the RINEPT spectrum acquired with phase cycling (Fig. 9C) is of good quality, this method has some disadvantages for our purposes. As shown in the previous sections, the MR signals of molecules with more than two coupled spins still have components that are not enhanced by polarisation transfer when acquired with RINEPT. These signal components still contribute to the overall signal when acquired with proton decoupling but cancel out when using phase cycling. Thus, the signal enhancement of refocused INEPT is about 10–30% lower when phase cycling is used (Fig. 9B, C). Since the residual signal of the uncoupled metabolites in spectra acquired without phase cycling does not disturb the post-processing, this sequence is preferred due to the higher signal yield.

Discussion/conclusion

This report describes theory and experimental observations of ^{31}P signal enhancements through heteronuclear polarisation transfer with the RINEPT experiment. It demonstrates that RINEPT amplifies the signal of coupled ^{31}P–^{1}H spin systems in aqueous model solutions

and in vivo. The measured signal enhancements of metabolites with heteronuclear *J*-coupling in vivo varied from 0% (PE) to 163% (GPE) and differed between the experiments (Figs. 8 and 9). The reason for this variance is the difficult post-processing of the spectra obtained with Ernst-angle excitation, particularly in the range of the phospholipid signal. In contrast, the variation between different refocused INEPT experiments is small. Longitudinal measurements of the same volunteer over 4 weeks with the RINEPT sequence showed variations <5% of the metabolite signal intensities (PE, GPE, GPC).

We explain the relatively small enhancement of PE by the short T_2 (^{31}P) or an unfavourable combination of T_1 (^{1}H) and T_1 (^{31}P) relative to the applied sequence parameters. This will possibly improve when more precise data on in-vivo ^{31}P relaxation times of the human brain are available.

The enhancement with RINEPT is remarkable for all metabolites with scalar ^{13}P–^{1}H coupling when comparing the spectra to those in which the signal is enhanced only by NOE (Fig. 9). The signal amplification with refocused INEPT exceeds that of NOE when using the typical parameters for in-vivo measurements (short *TR,* large *NEX*).

The determination of the echo times TE_1 and TE_2 in the experiments with solutions containing MDPA and PE as well as the observed signal enhancement with the RINEPT sequence were in good agreement with the calculations of the theoretical model for these spin systems. This confirmed that the poor synchronisation of the second RF channel has no detectable effect on the double-resonance experiments when using 1-ms rectangular pulses.

One theoretical argument against the use of RINEPT in vivo are the assumed short T_2 times of the endogenous ^{31}P spins. The values of these constants in the literature range from 10 ms to more than 80 ms [1, 3, 4, 12]. Our results show that even though the required echo times for the RINEPT experiment are quite long, there is still a large signal enhancement compared to conventional methods. From the observation of enhancement with *TE*=40 ms and of narrow spectral line widths of GPE, GPC, and PE resonances (range: 4.9–7 Hz) we conclude that the in-vivo T_2 times of these metabolites must be larger than expected.

Besides the enhancement through polarisation transfer, an additional signal amplification is obtained for short *TR* in the order of T_1^H of the protons. The maximum of this relaxation-dependent enhancement was found with *TR*=1.2–1.7 s, which is nearly the minimum repetition time the SAR monitor permits for in-vivo ^{31}P MR spectroscopy with ^{1}H-decoupling. Nevertheless, these values need further investigation through measurement of T_1^H in subsequent studies. Another advantage of RINEPT is that the long echo times allow application of phase encoding gradients for MR spectroscopic imaging.

A limitation of the RINEPT method is that only information on metabolites with scalar ^{1}H–^{31}P coupling can be acquired. However, there is strong interest to detect and quantify in-vivo ^{31}P MR signals of PME and PDE. Altered concentrations of these compounds have been hypothesised and observed in many ^{31}P studies, e. g., of schizophrenic patients [13, 14, 15, 16, 17], depressive/bipolar patients [18, 19], Alzheimer patients [20, 21], and in patients with tumours [22, 23]. The simplified RINEPT spectra are easier to quantify than ^{31}P spectra obtained with more conventional methods which facilitates the analysis and comparison of longitudinally acquired intra-individual spectra as well as inter-individual comparisons of theses signals.

Acknowledgements The authors thank Gerald Matson (UCSF, San Francisco) for building the double-tuned head coil and William E. Hull (DKFZ, Department: Central Spectroscopy) for the acquisition and interpretation of high-resolution MR spectra from MDPA and PE.

References

1. Gonen O, Mohebbi A, Stoyanova R, Brown TR (1997) In vivo phosphorus polarization transfer and decoupling from protons in three-dimensional localized nuclear magnetic resonance spectroscopy of human brain. Magn Reson Med 37:301–6
2. Payne GS, Leach MO (2000) Surface-coil polarization transfer for monitoring tissue metabolism in vivo. Magn Reson Med 43:510–6
3. Lara RS, Matson GB, Hugg JW, Maudsley AA, Weiner MW (1998) Quantitation of in vivo phosphorus metabolites in human brain with magnetic resonance spectroscopic imaging (MRSI). Magn Reson Imaging 1993;11:273–8
4. de Graaf RA (1998) In vivo NMR spectroscopy. Wiley, West Sussex
5. Richardson AJ, Allen SJ, Hajnal JV, Cox IJ, Easton T, Puri BK (2001) Associations between central and peripheral measures of phospholipid breakdown revealed by cerebral 31-phosphorus magnetic resonance spectroscopy and fatty acid composition of erythrocyte membranes. Prog Neuropsychopharmacol Biol Psychiatry 25:1513–21
6. Burum DP, Ernst RR (1980) Net polarization transfer via a J-ordered state for signal enhancement of low-sensitivity nuclei. J Magn Reson 39:163–168
7. Morris GA, Freeman R (1979) Enhancement of nuclear magnetic resonance signals by polarization transfer. J Am Chem Soc 101:760–762
8. Matson GB, Vermathen P, Hill TC (1999) A practical double-tuned ^{1}H/^{31}P quadrature birdcage headcoil optimized for ^{31}P operation. Magn Reson Med 42:173–82

9. Luyten PR, Bruntink G, Sloff FM, Vermeulen JW, van der Heijden JI, den Hollander JA, Heerschap A (1989) Broadband proton decoupling in human ^{31}P NMR spectroscopy. NMR Biomed 1:177–83
10. Smith SA (1999) GAMMA users manual. http://gamma.magnet.fsu.edu
11. Vanhamme L, van den Boogaart A, Van Huffel S (1997) Improved method for accurate and efficient quantification of MRS data with use of prior knowledge. J Magn Reson 129:35–43
12. Kilby PM, Allis JL, Radda GK (1990) Spin-spin relaxation of the phosphodiester resonance in the ^{31}P NMR spectrum of human brain. The determination of the concentrations of phosphodiester components. FEBS Lett 272:163–5
13. Deicken RF, Calabrese G, Merrin EL, Meyerhoff DJ, Dillon WP, Weiner MW, Fein G (1994) ^{31}Phosphorus magnetic resonance spectroscopy of the frontal and parietal lobes in chronic schizophrenia. Biol Psychiatry 36:503–510
14. Shioiri T, Kato T, Inubushi T, Murashita J, Takahashi S (1994) Correlations of phosphomonoesters measured by phosphorus-31 magnetic resonance spectroscopy in the frontal lobes and negative symptoms in schizophrenia. Psychiatry Res 55:223–35
15. Volz HP, Rzanny R, Rossger G, Hubner G, Kreitschmann-Andermahr I, Kaiser WA, Sauer H (1998) ^{31}Phosphorus magnetic resonance spectroscopy of the dorsolateral prefrontal region in schizophrenics - a study including 50 patients and 36 controls. Biol Psychiatry 44:399–404.
16. Bluml S, Tan J, Harris K, Adatia N, Karme A, Sproull T, Ross B (1999) Quantitative proton-decoupled^{31}P MRS of the schizophrenic brain in vivo. J Comput Assist Tomogr 23:272–5
17. Potwarka JJ, Drost DJ, Williamson PC, Carr T, Canaran G, Rylett WJ, Neufeld RW (1999) A^{1} H-decoupled ^{31}P chemical shift imaging study of medicated schizophrenic patients and healthy controls. Biol Psychiatry 45:687–93
18. Volz HP, Rzanny R, Riehemann S, May S, Hegewald H, Preussler B, Hubner G, Kaiser WA, Sauer H (1998) ^{31}P magnetic resonance spectroscopy in the frontal lobe of major depressed patients. Eur Arch Psychiatry Clin Neurosci 248:289–95
19. Yildiz A, Sachs GS, Dorer DJ, Renshaw PF (2001) ^{31}P nuclear magnetic resonance spectroscopy findings in bipolar illness: a meta-analysis. Psychiatry Res 106:181–91
20. Gonzalez RG, Guimaraes AR, Moore GJ, Crawley A, Cupples LA, Growdon JH (1996) Quantitative in vivo ^{31}P magnetic resonance spectroscopy of Alzheimer disease. Alzheimer Dis Assoc Disord 10:46–52
21. Smith CD, Pettigrew LC, Avison MJ, Kirsch JE, Tinkhtman AJ, Schmitt FA, Wermeling DP, Wekstein DR, Markesberry WR (1995) Frontal lobe phosphorus metabolism and neuropsychological function in aging and in Alzheimer's disease. Ann Neurol 38:194–201
22. Podo F (1999) Tumour phospholipid metabolism. NMR Biomed 12:413–39
23. Maintz D, Heindel W, Kugel H, Jaeger R, Lackner KJ (2002) Phosphorus-31 MR spectroscopy of normal adult human brain and brain tumours. NMR Biomed 15:18–27